8–10

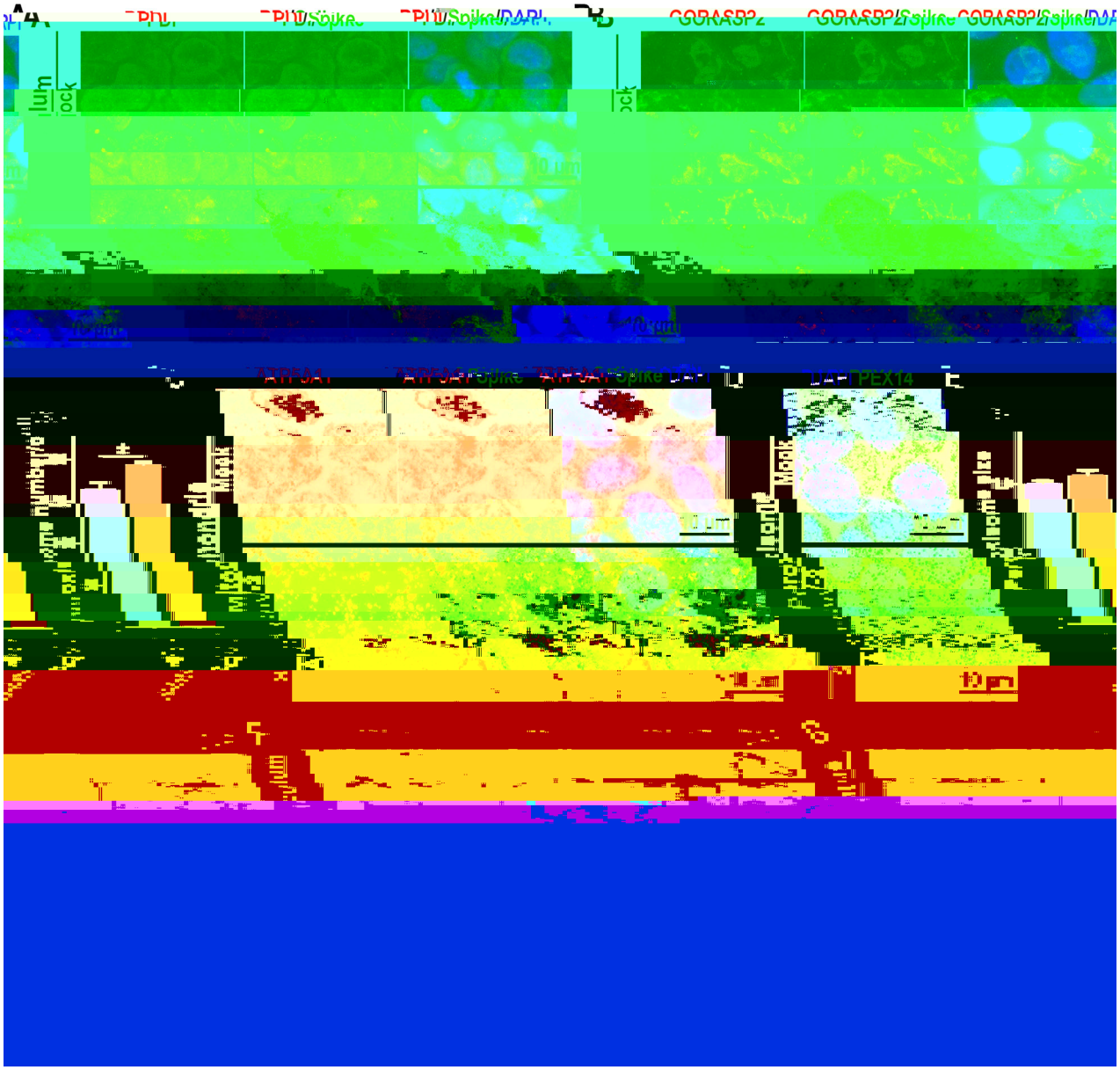

Fig. 2 Organelles of HPAEpiC cells and HULEC-5a cells following SARS-CoV-2 infection. a Representative images of endoplasmic reticulum immunostained with anti-PDI antibody for mock- or SARS-CoV-2-infected HPAEpiC cells. The white arrows indicated the co-localization of virus particles and endoplasmic reticulum within the host cells. **b** Representative images of Golgi apparatus immunostained with anti-GORASP2 antibody for mock- or SARS-CoV-2-infected HPAEpiC cells. **c** Representative images of mitochondria immunostained with anti-ATP5A1 antibody for mock- or SARS-CoV-2-infected HPAEpiC cells. **d** Representative images of peroxisomes immunostained with anti-PEX14 antibody for mock- or SARS-CoV-2-infected HPAEpiC cells. **e** Quantification of peroxisome size and density (number/cell) for mock- or infected cells in (**d**). Data were analyzed by Student's *t* test (*: $P < 0.05$). Data represent four independent experiments, and more than 150 cells for each group were quantified. Data were presented as mean ± SEM. **f** Representative images of mitochondria and endoplasmic reticulum of mock- or SARS-CoV-2-infected HULEC-5a cells. **g** Representative images of peroxisomes and Golgi apparatus of mock- or SARS-CoV-2-infected HULEC-5a cells. All results are representative for three independent experiments.

A, -C - 2- HPAE C H LEC-5 (F, . 3) G E- (F, . 3) H LEC-5 . A A, -C -2 E-

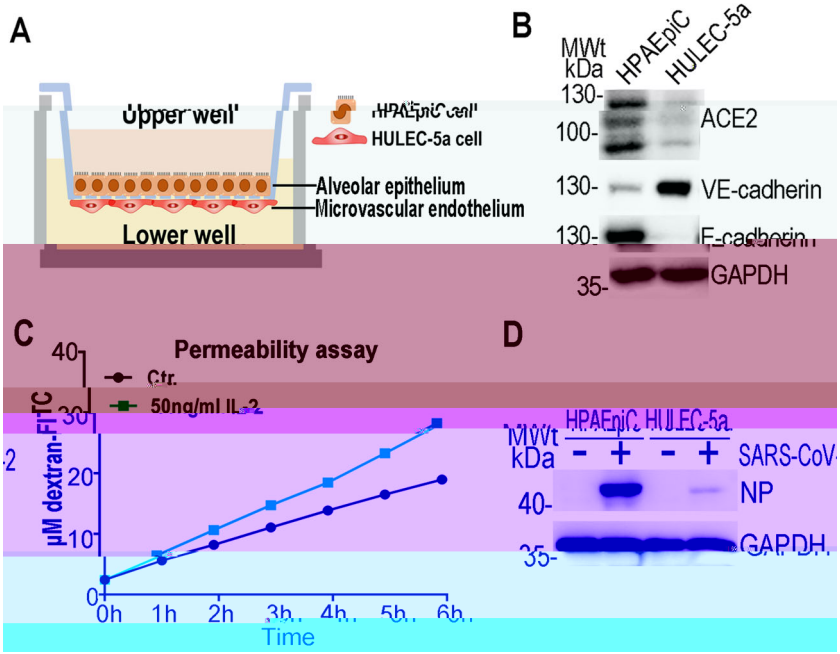

Fig. 4 SARS-CoV-2 infection in an alveolar epithelium/endothelium co-culture system based on transwell. a A schematic diagram for an alveolar epithelium/endothelium co-culture system based on a transwell chamber. **b** Western blot was performed to analyze the levels of ACE2, E-cadherin (epithelial cell marker), and VE-cadherin (vascular endothelial cell marker) for HPAEpiC cells and HULEC-5a cells collected from the co-culture system, separately. **c** Blood-to-alveolus permeability assay of dextran-FITC (10 kDa) was measured on the co-culture system to evaluate the integrity of the alveolar–capillary barrier. Data were presented as mean ± SEM, $n = 3$. Data were analyzed by Student's t test (***: $P < 0.001$). **d** Western blot was performed to analyze the viral Nucleoprotein (NP) level of HPAEpiC cells and HULEC-5a cells collected from the co-culture system separately following SARS-CoV-2 infection. **b**, **d** These results are representative blots from three independent experiments.

, HPAE C, H LEC-5 (F . 4).

(HPAE C E-) (F . 4). I -FI C (10 D)

. A F . 4 , -FI C IL-2.

A -C -2 MOI 10. A 72 , N (NP) NP HPAE C H LEC-5 (F . 4), fi fi HPAE C H LEC-5 (F . 1 –). A fi NP.

CO ID-19 [3].

Define the proteomic response of host cells to SARS-CoV-2 infection

. B fl , 72 , HPAE C H LEC-5 – (LC–M / M) (F . 5). H, (IM) -fl (OF) . B I . 2017.

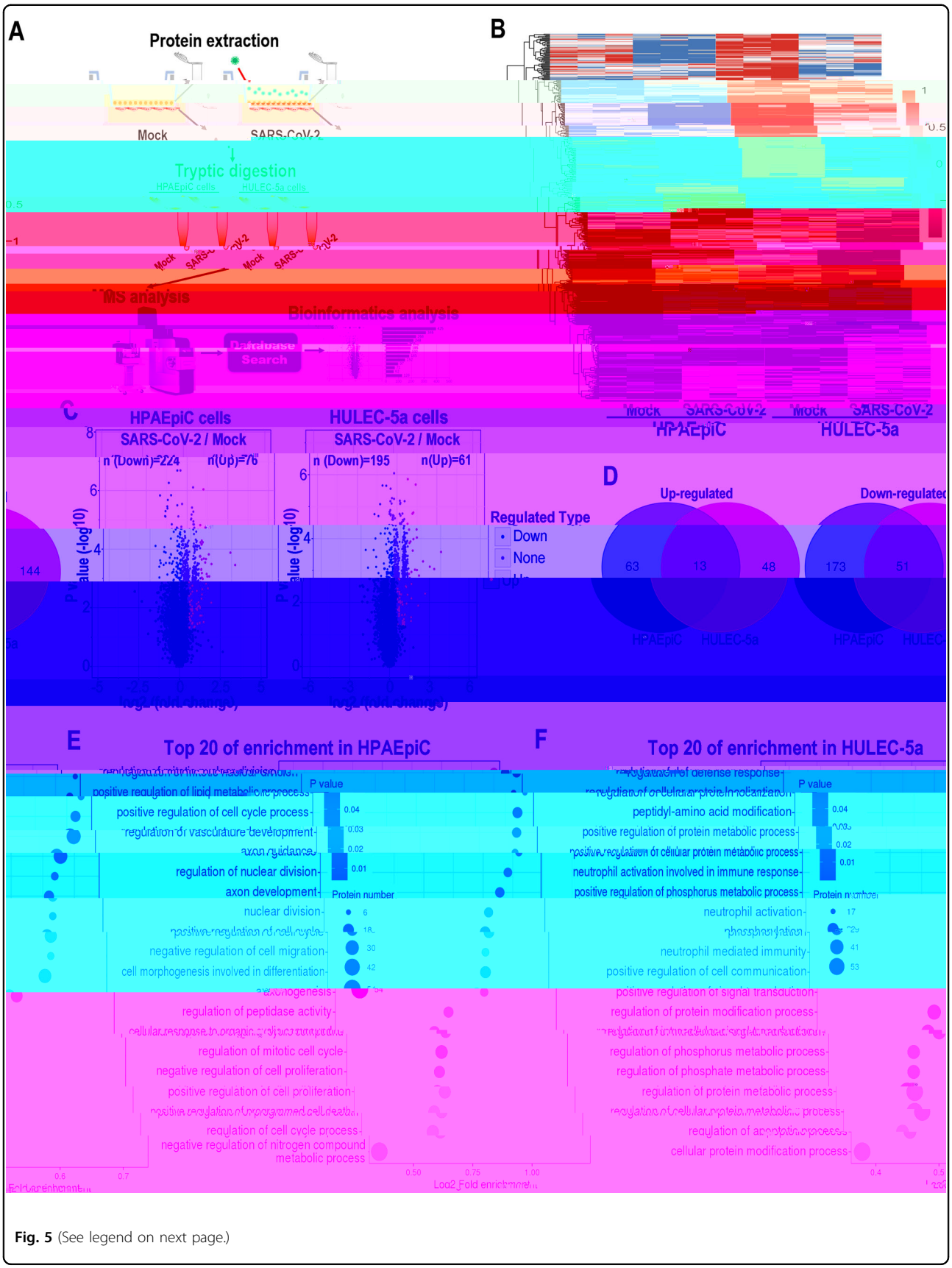

Fig. 5 (See legend on next page.)

M /M IM
[24,25].
, 6546 fi , 6011
fi . H A -C -
2 -
HPAE C H LEC-5 (F . 5). F
fi (DEP),
P-
1.5 0.05, . P
. A DEP , 300 (76 -
224 -)
fi HPAE C
(F . 5 ; 1); , 256 (61
- 195 -)
fi H LEC-5
(F . 5 ; 2). B
64 DEP , ~1%
fi , HPAE C
H LEC-5 A -C -2 -
(F . 5).
fi A -
C -2 , G O
fi . .
GO
HPAE C H LEC-5
(F . 5 ,). A 20 GO
HPAE C .
, H LEC-5 , -
, fi
.
G , A -C -2 -

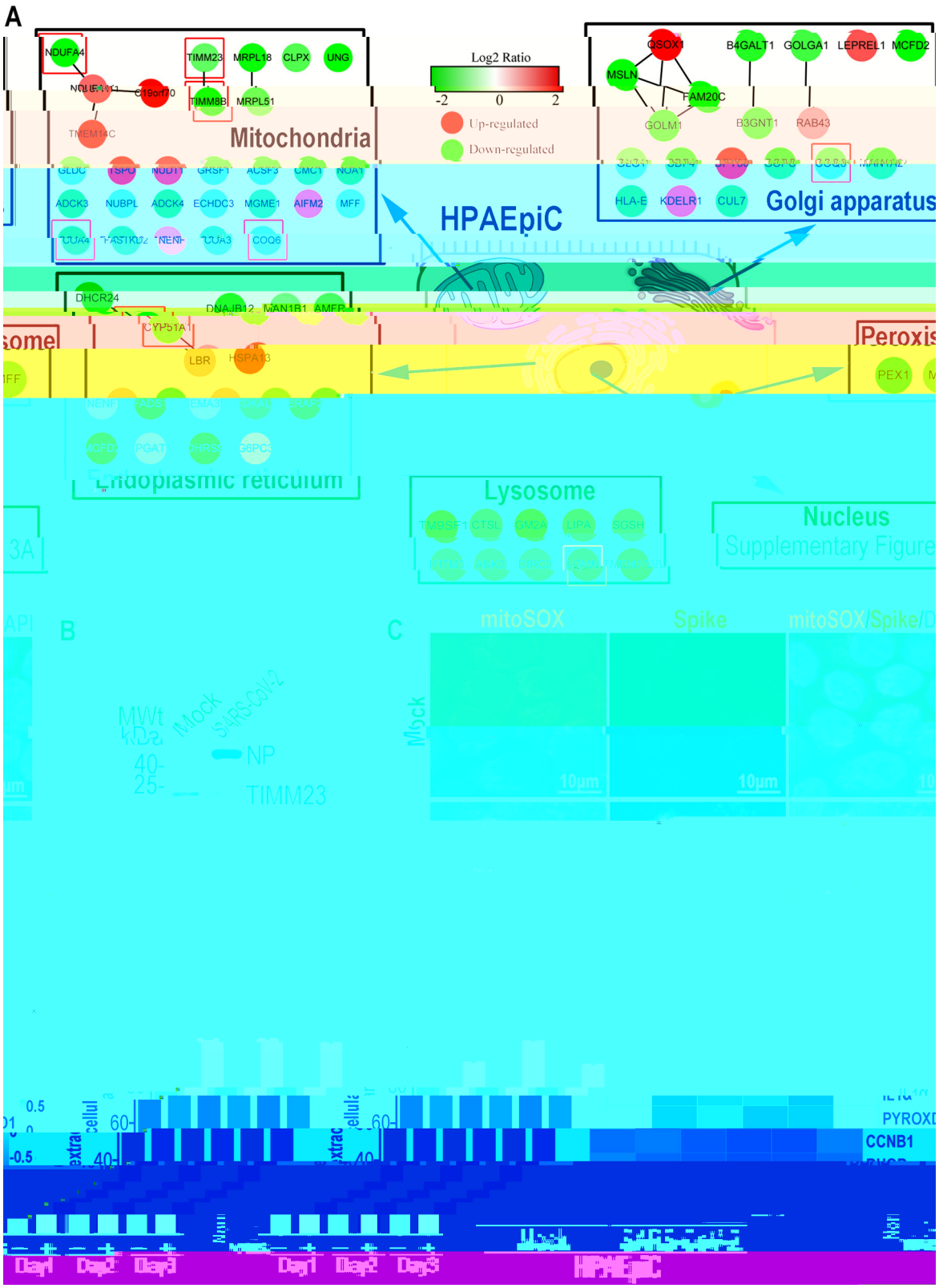

Fig. 6 (See legend on next page.)

A -C -2 (F . 4A, B).
I , , 5 .
(F . 6). ND FA4
I , COA4
I [27–29]. IMM23 -
[30,31]. A
, HIAE C
ND FA4 IMM23 -
(F . 6).
M (O), -
O , -
[32–34].
O - A -C -2- HIAE C
O fl (-
O). A F . 6 , ,
- HIAE C , O
fi A -C -2- . I
O
[35,36]. ,
O
HIAE C H LEC-5 -
ELI A . O (>
0.05) HIAE C (F . 6);
O H LEC-5
(F . 6). O
H LEC-5 . A , .
fi

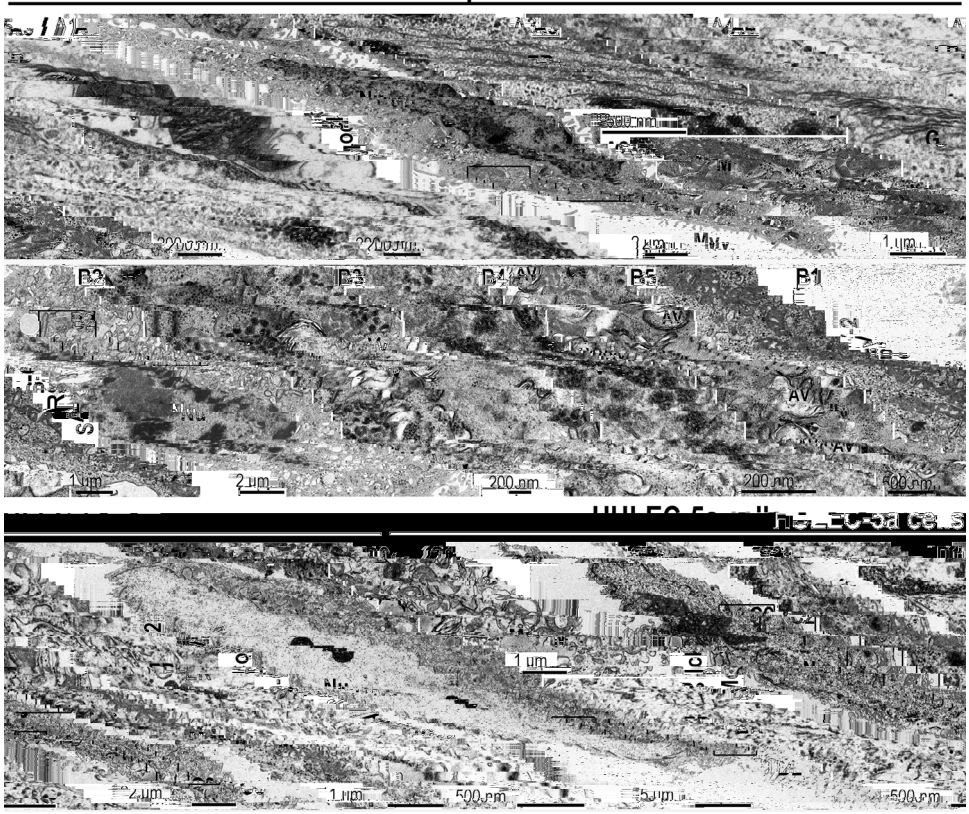

Fig. 7 TEM analysis of mock- and SARS-CoV-2-infected cells from alveolar co-culture system. a TEM micrographs of HPAEpiC cells of mock-infected group. **a1** The overall image of the HPAEpiC cell. The area indicated by black box was enlarged in **a2**. **a2** The micrograph of mitochondria (M) of HPAEpiC cell. **a3** The micrograph of smooth endoplasmic reticulum (ER) of HPAEpiC cell. **a4** The micrograph of Golgi apparatus (G) of HPAEpiC cell. **a5** The micrograph of lamellar body (LB) within cell body. **b** TEM micrographs of HPAEpiC cells of SARS-CoV-2-infected group. **b1** The overall image of the infected cell. The area indicated by the black box is enlarged in **b2**. **b2** The micrograph of clusters of virus particles (V) within cell body. **b3** Enlarged image of virus indicated in **b2**. **b4** A large amount of autophagic vacuoles (AV) in the infected HPAEpiC cells. **b5** The micrograph of fragmented mitochondria (M) in the infected HPAEpiC cells. **c** TEM micrographs of HULEC-5a cells of mock-infected group. **c1** The overall image of the HULEC-5a cells. The areas indicated by black boxes were enlarged in **c2** and **c3**, respectively. **c2** The micrograph of mitochondria in the mock-infected HULEC-5a cells. **c3** The micrograph of rough endoplasmic reticulum (ER) in mock-infected HULEC-5a cells. **d** TEM micrographs of HULEC-5a cells of SARS-CoV-2-infected group. **d1** The overall image of the HULEC-5a cells. The areas indicated by black box were enlarged in **d2**. **d2** The micrograph of fragmented mitochondria (M) with swollen cristae in HULEC-5a cells of SARS-CoV-2-infected group. **d3** The micrograph of dilated rough endoplasmic reticulum (ER) in HULEC-5a cells of SARS-CoV-2-infected group. Nu: nucleus; Mv: microvilli; M: mitochondria; ER: endoplasmic reticulum; G: Golgi apparatus; LB: lamellar body; V: virus particle; AV: autophagic vacuole. Three independent experiments were performed ($n = 3$).

H LEC-5 - (F . 7 ,). C , EM , A , -C -2 - HPAE C , , H LEC-5 , - , A , -C -2 - , ,

Daurisoline, an autophagy inhibitor, could inhibit SARS-CoV-2 replication in host cells

A HPAE C , A , -C -2 [19] fi HPAE C A , -C -2 (F . 5). - . F , (4), , D , fi

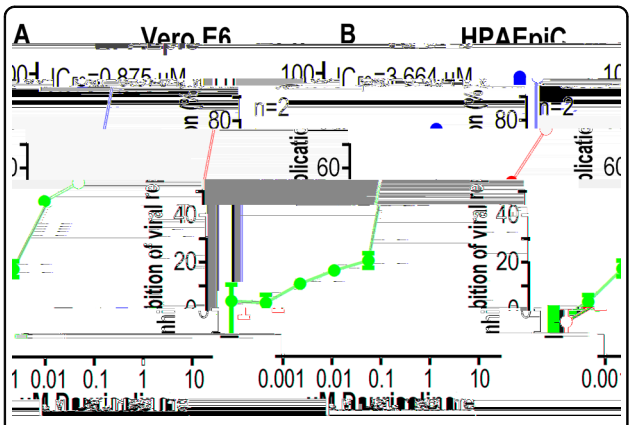

Fig. 8 Daurisoline could inhibit SARS-CoV-2 replication in Vero E6 cells and HPAEpiC cells. a Antiviral assay showed inhibition of viral replication in dependency of Daurisoline concentration in Vero E6 cells ($n = 2$). **b** Antiviral assay showed inhibition of viral replication in dependency of Daurisoline concentration in HPAEpiC cells ($n = 2$).

E6 (F . 8). D HPAE C (F . 8). D (M) [42,43].

Discussion

I fi A -C -2 CO ID-19. I A -C -2 A -C -2 G N . B A -C A -C fi [44]. G A -C -2 A -C A -C -2 A -C . B P [45]. A 1, [45]. A A -C -2 . B G fi A -C -2 [13,14]. H A -C 2 . P . A fi fi (. IL1α I G15). C A -C -2 (. IL1α IFN) A A -C -2 DEP A -C -2 G . G fi . B [26], fi 13 DEP HPAE C C -2 A -C -2 . I , fi fi A -C -2 fi ND FA4 IMM23

HPAE C , A , -C -2 . A , fl O . A , O IL1α[37,38]. H , A , -C -2 O , O IL1α C , EM , A , -C -2 - , A , -C -2 . N . P , D . O , O A , -C -2 - , - , - . fi , –

Materials and methods

Cell culture

E6 A C C (A CC, . 1586) MEM (G) 10% (FB ; G). I (HPAE C) II (- C) PMI 1640 (G) 10% FB (G) 1% P/ . H LEC-5 P C (A CC C), H LEC-5 (P , CM-0565). A 37 C fi 5% CO_2. A fi .

Virus preparation and viral titer determination

A , A , -CO -2 107, G P C D C P , G P C , E6 , CID50 E6 . A -3 (B L-3) .

SARS-CoV-2 infections

C 35 - 48- , 24 , , A , -C -2 MOI 10. O , PB 3 . O 3 . - , NA , fi 4% PFA fl . F , A , -C -2 , 1 L PMI 1640 (MOI = 10) . O , PB . O 3 - , .

Antibodies, reagents, and lab consumables

A -ACE2 (21115-1-AP), - MP , 2 (14437-1-AP), -E- (60335-1-I), - E- (66804-1-I), -GO A P2 (66627-1-I), -PDI (66422-1-I), -A P5A1 (66037-1-I), - A P5A1 (14676-1-AP), -PE 14 (10594-1-AP) - IMM23 (11123-1-AP) P G . A -ND FA4 (3008) I . A -GAPDH (C 0100) - C BIO . A - (40150- 007) -N (40143- 019) B . - 4. L G J. B -F C ., L .

Western blot analysis

P 10% D -PAGE 0.2 μ (GE A). A 5% B A B 0.05% -20, 4 C . (H P)- - 1 . P P B D (GE).

Determination of virus titers using qRT-PCR

O NA HP NA K (, C . 11858882001)

-PC . - PC (A. B , A™ 7) O , . -PC NA PC (O OBO, -101A). PC : N-F: 5′-GGGGAAC C CC GC A-GAA -3′; N- : 5′-CAGACA GC C CAAGC G-3′; N. . : 5′- GC GC GC GACAGA -3′. PC . fi : 50_C 10 , 95_C 1 45 95_C 15 , 60_C 45 .

Immunofluorescent staining

C fi 4% . (PFA) 4_C . , PB , . PB (0.2% -100 PB) 5% 30 . A PB . C . 4_C . 1 . A , DAPI . I C L, M880 fl .

Co-culture of cells on the transwell chamber

C - (6 .) 0.4 µ . fi (C I .) . - fi [46]. B , - . I (1:50) 48 , . PB . P 6 . . H LEC-5 . 1. 10^6, 2 . P 6 . , H LEC-5 . 5. 10^6 HPAE. C . 24 .

Permeability assay of alveolar–capillary barrier

H LEC-5 HPAE. C . 24 , . H LEC-5 50 / L IL-2 4 . HPAE. C H LEC-5 PMI1640 . A , 100 µM -FI C ( ). -FI C . ( ) . (0 , 1 , 2 , 3 , 4 , 5 , 6) . –

Antiviral assay

F E6 , E6 CCK8 (B , C). B fl , E6 . 96- . 24 . E6 , A , -C -2 MOI 0.1. MEM 2% FB . 1 , – . A 72 , CCK8 , 50% (IC50) O P. 2016 .

F HPAE. C , . PC . B fl , HPAE. C . 48- . 24 . HPAE. C , A , -C -2 MOI 10. PMI 1640 10% FB . 1 , – . A 72 , NA PC .

Mitochondrial ROS detection assay

HPAE. C 35 (2. 10^6) PMI 1640 10% FB . A 24 , A , -C -2 MOI 10. O , PB 3 . O 3 . - , O 20 37_C. A PB , fi 4% . - (PFA) 20 . B , DAPI .

Transmission electron microscopy

HPAE. C H LEC-5 , fi PB , 4% PFA (E M .) 2.5% (E M .) 4_C . A PB fi 1% O O4 . 2 , - , E 812 (PI). (70) 2% 30 10 . I JEM-1400PL , .

Protein extraction and trypsin digestion for quantitative mass spectrometry

C , ,

B L-3 . I , J P M B L (H -) C . L ( ) 12,000 *g* 4 C 10 . F , BCA ' .

F 5 M 30 56 C 11 M 15 - 100 M EAB (2 M). F , 1:50 - fi 1:100 - 4 - .

Analysis by liquid chromatography-mass spectrometry

A (0.1% , 2% /), (25- , 75/100 µ . .). P 6% 24% B (0.1%) 70 , 24% 35% 14 80% 3 80% 3 , fl 450 L/ E HPLC (B D).

C OF P (B D) . 1.75 . P OF , M /M 100 1700 /. OF P - (PA EF) . P 0 5 , 10 PA EF-M /M 30 .

Database search

M /M M - (.1.6.6.0). KA158L (20395) . /P fi - 20. F 20. M , 20. . C - C . fi fi fi , N- M fi fi . FD <1%.

Proteome annotation

G O (GO) P -GOA (:// / GOA/). F , fi ID P ID GO ID ID. I fi P - GOA , I P 5.36 ' GO . P I P I P (75.0) . K E - G G (KEGG). - (:// / /) . F , KEGG KAA (:// / - / /) ' KEGG . KEGG KEGG (:// / /). E K O G KOG BLA 2.2.31 - 1 -5. - P KB (:// / /).

Identification of differentially expressed proteins (DEPs)

LF . fi . C - , fi - fi - 2 ( ), - - *T*- .

Functional enrichment

F GO KEGG. , - F ' " " fi . GO KEGG. - < 0.05 fi .

Enrichment-based clustering

F fi , GO, D , KEGG. A - , -

< 0.05 fi . fi - = – 10 (-). F , - (E , -) G . C “ .2” “ ”.

Protein–protein Interaction Network

A - ING 11.0 (://- /) . O . ING fi “ fi ” fi . H , fi >0.7 (fi). I ING C 3.8.0 . I DEP C 3.8.0 .

Statistical analyses

D E (M) . G P P 6 . A . D . D ’ . M - (ANO A) B . (EM). fi : *, $P < 0.05$; **, $P < 0.01$; ***, $P < 0.001$.

Acknowledgements

The authors thank Prof. Yonggang Yao (Kunming Institute of Zoology, CAS) for his strong support on this work. We thank the Kunming Biological Diversity Regional Center of Instruments, Kunming Institute of Zoology, CAS for our electron microscopy work, and we are grateful to Yingqi Guo for her help with preparing EM samples. We thank Can Peng (Center for Biological Imaging (CBI), Institute of Biophysics, Chinese Academy of Science) for her advice on EM samples preparation. We thank Jingjie PTM BioLab (Hangzhou) Co. Ltd for their service on mass spectrometry analysis of the protein samples. This research was supported by the Strategic Priority Research Program of the Chinese Academy of Sciences, Grant (Nos. XDB29050301, XDA16020900, XDB32030200), National Key R&D Program of China (Nos. 2020YFC0842000, 2017YFB0405404), National Science and Technology Major Project (No. 2018ZX09201017-001-001), National Nature Science Foundation of China (Nos. 31671038, 31971373, 81703470, 81803492), Innovation Program of Science and Research from the DICP, CAS (DICP I201934), China Postdoctoral Science Foundation (No. 2019M660065) and Yunnan Key Research and Development Program (202003AD150009).

Author details

[1]Division of Biotechnology, CAS Key Laboratory of SSAC, Dalian Institute of Chemical Physics, Chinese Academy of Sciences, Dalian, China. [2]Kunming National High-level Bio-safety Research Center for Non-human Primates, Center for Biosafety Mega-Science, Kunming Institute of Zoology, Chinese Academy of Sciences, Kunming 650107, China. [3]Key Laboratory of Animal Models and Human Disease Mechanisms of Chinese Academy of Sciences, KIZ-CUHK Joint Laboratory of Bioresources and Molecular Research in Common Diseases, Kunming Institute of Zoology, Chinese Academy of Sciences, Kunming, Yunnan 650223, China. [4]University of Chinese Academy of Sciences, Beijing, China. [5]Key Laboratory of Animal Models and Human Disease Mechanisms of Chinese Academy of Sciences, Kunming Institute of Zoology, Chinese Academy of Sciences, Kunming 650223 Yunnan, China. [6]CAS Center for Excellence in Brain Science and Intelligence Technology, Chinese Academy of Sciences, Shanghai, China. [7]Institute for Stem Cell and Regeneration, Chinese Academy of Sciences, Beijing, China

Data availability

All relevant data are available in the manuscript or supplementary information. The mass spectrometry proteomics data have been deposited to the ProteomeXchange Consortium via the PRIDE partner repository with the dataset identifier PXD020470.

Conflict of interest

The authors declare that they have no conflict of interest.

Publisher's note

Springer Nature remains neutral with regard to jurisdictional claims in published maps and institutional affiliations.

Supplementary Information accompanies this paper at (https://doi.org/10.1038/s41419-020-03252-9).

Received: 11 August 2020 Revised: 15 November 2020 Accepted: 17 November 2020
Published online: 08 December 2020

References

1. Xu, Z. et al. Pathological findings of COVID-19 associated with acute respiratory distress syndrome. Lancet. *Respir. Med.* **8**, 420–422 (2020).
2. Wichmann, D. et al. Autopsy findings and venous thromboembolism in patients With COVID-19. *Ann. Intern. Med.* https://doi.org/10.7326/M20-2003 (2020).
3. Zhang, H. et al. Histopathologic changes and SARS-CoV-2 immunostaining in the lung of a patient with COVID-19. *Ann. Intern. Med.* **172**, 629–632 (2020).
4. Goshua, G. et al. Endotheliopathy in COVID-19-associated coagulopathy: evidence from a single-centre, cross-sectional study. *Lancet Haematol.* https://doi.org/10.1016/S2352-3026, 30216-30217 (2020).
5. Zhou, H. S. et al. Lipopolysaccharide impairs permeability of pulmonary microvascular endothelial cells via Connexin40. *Microvasc. Res.* **115**, 58–67 (2018).
6. Pober, J. S. & Sessa, W. C. Evolving functions of endothelial cells in inflammation. *Nat. Rev. Immunol.* **7**, 803–815 (2007).
7. Chan, M. C. et al. Influenza H5N1 virus infection of polarized human alveolar epithelial cells and lung microvascular endothelial cells. *Respir. Res.* **10**, 102 (2009).
8. Sun, J. et al. Isolation of infectious SARS-CoV-2 from urine of a COVID-19 patient. *Emerg. Microbes Infect.* **9**, 991–993 (2020).

14. Jean Beltran, P. M., Mathias, R. A. & Cristea, I. M. A portrait of the human organelle proteome in space and time during cytomegalovirus infection. *Cell Syst.* **3**, 361–373 e366 (2016).
15. Ostaszewski, M. et al. COVID-19 Disease Map, building a computational repository of SARS-CoV-2 virus-host interaction mechanisms. *Sci. Data* **7**, 136